Received: March 23, 2019

INASS

International Journal of
Intelligent Engineering & Systems

http://www.inass.org/

Sensorless Control for High Performance SPIM Drives Based on the Improved Rotor Flux Identifier Using Sliding Mode

Ngoc Thuy Pham[1]* **Khuong Huu Nguyen[2]**

[1]*Department of Electrical Engineering Technology,*
Industrial University of Ho Chi Minh City, Vietnam
[2]*Department of Telecommunication - Electronics and Electrical Engineering,*
Ho Chi Minh City University of Transport, Vietnam
* Corresponding author's Email: ngocpham1020@gmail.com

Abstract: In this paper, a novel Stator Current Based Model Reference Adaptive System (SC_MRAS) speed estimation scheme using neural network (NN) and Sliding Mode (SM) is proposed to improve the performance of the MRAS speed observer for high-performance Six Phases Induction Motor (SPIM) drives, especially at low and zero speed region, where the poor performance of observers is still always a large challenge. In this paper, a two-layer linear NN, which has been trained online by means of the Least Squares (LS) algorithm, is used as an adaptive model to estimate the stator current and this model is employed in prediction mode. These novel proposed can ensure that the whole drive system achieves faster satisfactory torque and speed control and strong robustness, the observer operate better accuracy and stability both in transient and steady-state operation. Especially, in this proposed observer, the rotor flux, which is needed for the stator current estimation of the adaptive model and providing to the controller, is identified based on adaptive SM technique. The improvement of Rotor Flux Estimation for SC_MRAS-Based Sensorless SPIM Drives help to eliminate the disadvantages in SC_MRAS based observer such as stator resistance sensitivity, and flux open loop integration which may cause dc drift and initial condition problems or instability in the regenerating mode of operation, therefore, enhancing the rotor flux estimation, speed estimation and control accuracy at very low and zero stator frequency operation help improve the observer and overall drive system performance. The indirect field oriented control (IFOC) for speed control of a sensorless SPIM drive using the proposed observer is built by MATLAB/ Simulink. The simulation results have proven that the observer give the good dynamic performance, quick convergence, low estimation errors both in transient and steady state operation. The proposed sensorless increase the system's accuracy, reliability and robustness. Parameter sensitivity, computational effort and stability at low and zero speed are significantly improved.

Keywords: Neural network, Sensorless vector control, Six phase induction motor drive, MRAS observer.

1. Introduction

In the past decades, multiphase motor drives have been proposed for applications [1–3] due to its advantages are such as: decrease the single switches current stress instead of adopting parallel techniques, low electromagnetic torque pulsations, DC link current harmonics, overall system reliability and better power distribution per phase improve the overall system reliability [3]. Among the different control solutions for SPIM drives, one of the most interesting and extensively discussed in the literature is SPIM having two sets of three-phase windings spatially shifted by 30 electrical degrees. Neutral points of the two windings can be isolated or connected. The major reason for selecting the asymmetrical six-phase winding instead of the true six-phase winding (60° displacement between any two consecutive phases) was the elimination of the sixth harmonic from the torque [3], which is important in six-phase IM drives using voltage source inverter (VSI) with six-step operation.

In order to regulate the SPIM in high performance applications several control techniques

have been developed being the field oriented control method [1] one of the most popular techniques. The correct knowledge of rotor speed information for field orientation is required. Moreover, the precise speed signal for closed-loop control is needed; therefore, speed encoders are essential to be mounted on the rotor shaft for position and speed information [4]. However, the encoder causes extra cost, larger size, and extra wiring of IM drives and limits their applications in a relatively harsh environment. In recent years, the development of sensorless IM drives without encoders or sensors have becoming more and more popular due to their advantages of minimizing production costs and developing a reliable and robust control system. Sensorless techniques are employed in hostile environments and also for emergency operations in safety-critical applications in case of failure of the sensor. They usually are divided into two categories, the fundamental model based observers and anisotropies model based observers. Model-based estimation strategies include open-loop observers [5], sliding-mode observers [6], Extended Kalman Filter [7], Backstepping [8], model reference adaptive systems (MRAS) [9] and artificial intelligence (AI) [10]. Recent research also used predictive current control for sensorless IM drives [11]. Sensorless drives have been successfully applied in medium and high speed regions [12, 13], but low and zero speed operation is still a large challenge. In order to overcome these problems a high frequency voltage or current carrier were injected, needed to excite the saliency itself [14]. This method works well at low and near zero speed region. However, their major disadvantages are computational complexity, the need of external hardware for signal injection and the adverse effect of injecting signal on the machine performance. Due to its simplicity and ease of implementation the model based methods and especially MRAS based methods are, until now, the most widely used. The main problems associated with the low speed operation of model-based sensorless drives are related to machine parameter sensitivity, stator voltage and current acquisition, and flux pure integration problems [15-18].

Numerous MRAS have been proposed. Among them, the rotor flux MRAS first introduced by Schauder [19], Flux Backstepping Observer [20], both suffer from DC drift problems associated with pure integration and sensitivity to stator resistance variation, especially in the low speed region. In order to improve the performance of observer overcome the effect by sensitivity to stator resistance variation, online adaptation of the stator resistance [21], the pure integration problems, Extended Kalman Filter (EKF), a modified torque based on MRAS schemes have proposed in [19], [20], respectively. Although [22, 23] have shown that these approaches significantly improve the performance of the RF-MRAS at low speed, these schemes remain the effected by the sensitivity to parameter variations. An improved rotor flux estimation to eliminate the pure integration problems and the effect of sensitivity to parameter variations for a Torque MRAS is proposed in [24]. Simulation and experimental results are shown the sensorless control drive operating at low and zero speeds, with both motoring and regenerative operations considered. The performance of the observer in low speed regenerating region and the performance of the transient and steady state were significantly improved at very low and zero rotor speeds. Analysis of the effect of parameter variation on the scheme performance has shown improved robustness against stator and rotor resistance variation over a wider range of load torques compared to results previously published for the conventional scheme. However, the estimated error increase at very low (3.14 rad/s) and zero speed range is recorded. The performance of the speed estimation in low speed regenerating region and the performance of the transient and steady state is not really satisfied.

Another approach, the stator current MRAS scheme has been introduced in [25-28]. [26] presents a stator current based MRAS speed observer using NN, which is an evolution of [25]. In this proposed scheme, to avoid the effect of a pure integrator and reduce influence of motor parameter variations, the measured stator current components are used as the reference model. The adaptive model of the proposed observer in [26] uses a two-layer NN with a BPN algorithm to estimate the rotor speed, an off-line trained multilayer feed-forward neural network is proposed as a rotor flux observer. The simulation and experimental results have proven that the significantly improvement operation performance in low and zero speed ranges, the lowest speed limit 25 rpm (2.6 rad/s) was reported. The results in [20] also demonstrate that the proposed observer can handle the parameter variation problem with a good level of robustness, sensorless performance with a 50% variation in resistances at low speed, 25% load. Although [26] can overcome the main problems associated with the low zero and speed operation, however, due to [26] the use of the nonlinear BPN algorithm to training a neural network causes some problem as local minima, paralysis of the neural network, need of two

heuristically chosen parameters, initialization problems, and convergence problems. These make the performance of observer in [26] is not really as expected. The speed estimation error and oscillation phenomenon at low and zero increase. Other side, the adaptive model in [26] is used in simulation mode, which means that its outputs are fed back recursively, this also make reduce the accuracy and stability of the responses of observer. Finally, the use of two networks: the first is online trained for stator current estimation and the second is off-line trained for rotor flux estimation will make increase the complexity and computational burden require high about hardware and time handle the data. This impose a large disadvantage of MRAS [26].

In this paper, a SC_MRAS based observer using NN and SM is proposed for improving the performance of the sensorless vector control SPIM drives, especially in low and zero speed ranges. the new points are developed in this SC_MRAS scheme are, first: Adaptive model uses a two layer linear neural network, which is trained online by a linear LS algorithm, this algorithm requires the less computation effort and overcome some drawbacks, which cause by its inherent nonlinearity as in literature published before [26], [28]. Second: the adaptive model based on NN is implemented in the prediction mode with no feedback loops between the output of the neural network and its input. This neural model is also used as a predictor with no feedback loops between the output of the neural network and its input. This improvement ensures the proposed observer operate better accuracy and stability, and especially, third: a rotor flux identifier, which is needed for the stator current estimation of the adaptive model and controller, is proposed based on SM. The gains are designed based on stability conditions of Lyapunov theory. This solution improves the rotor flux estimation accuracy, and consequently, the speed estimation accuracy at very low stator frequency operation. Finally, the modified Euler integration has been used in the adaptive model to solve the instability problems due to the discretization of the rotor equations of the machine enhance the performance of observer.

The indirect field oriented control (IFOC) for speed control of a sensorless SPIM drive using the proposed estimation algorithms is built by MATLAB/ Simulink. The theoretical analysis is validated by simulation tests of the sensorless SPIM drive system under different operating conditions. Tests are conducted and compare with benchmark tests based on [23-24, 29- 31]. The comparison data have proven that the proposed NN_SM_SC_MRAS observer are quicker convergence in speed estimation, better dynamic performances; lower estimation errors both in transient and steady-state operation. The terms of accuracy of the NN_SM_SC_MRAS observers is quite high and it is robustness against motor parameter variations. The paper is organized into five sections. In section 2, the basic theory of the model of the SPIM and the SPIM drive are presented. Section 3 introduces the proposed NN_SM_SC_MRAS observer. Simulation and discuss are presented in section 4. Finally, the concluding is provided in section 5.

2. Model vector control of SPIM drive

The system under study consists of an SPIM fed by a six-phase Voltage Source Inverter (VSI) and a DC link. A detailed scheme of the drive is provided in Fig.1. By applying the Vector Space Decomposition (VSD) technique introduced in [18], the original six-dimensional space of the machine is transformed into three two dimensional orthogonal subspaces in the stationary reference frame (D-Q), (x - y) and (zl -z2). This transformation is obtained by means of 6 x 6 transformation matrix:

$$T_6 = \frac{1}{\sqrt{3}}\begin{bmatrix} 1 & \frac{\sqrt{3}}{2} & -\frac{1}{2} & -\frac{\sqrt{3}}{2} & -\frac{1}{2} & 0 \\ 0 & \frac{1}{2} & \frac{\sqrt{3}}{2} & \frac{1}{2} & -\frac{\sqrt{3}}{2} & -1 \\ 1 & -\frac{\sqrt{3}}{2} & -\frac{1}{2} & \frac{\sqrt{3}}{2} & -\frac{1}{2} & 0 \\ 0 & \frac{1}{2} & -\frac{\sqrt{3}}{2} & \frac{1}{2} & \frac{\sqrt{3}}{2} & -1 \\ 1 & 0 & 1 & 0 & 1 & 0 \\ 0 & 1 & 0 & 1 & 0 & 1 \end{bmatrix} \quad (1)$$

In order to develop SPIM model for control purposes, some basic assumptions should be made. Hence, the windings are assumed to be sinusoidally distributed, the magnetic saturation, the mutual leakage inductances, and the core losses are neglected. The electrical matrix equations in the stationary reference frame for the stator and the rotor may be written as

$$\begin{aligned} [V_s] &= [R_s][I_s] + p([L_s][I_s] + [L_m][I_r]) \\ 0 &= [R_r][I_r] + p([L_r][I_r] + [L_m][I_s]) \end{aligned} \quad (2)$$

where: [V], [I], [R], [L] and [Lm] are voltage, current, resistant, self and mutual inductance vectors, respectively. *p* is differential operator. Subscript r and s related to the rotor and stator resistance respectively. Since the rotor is squirrel cage, [Vr] is

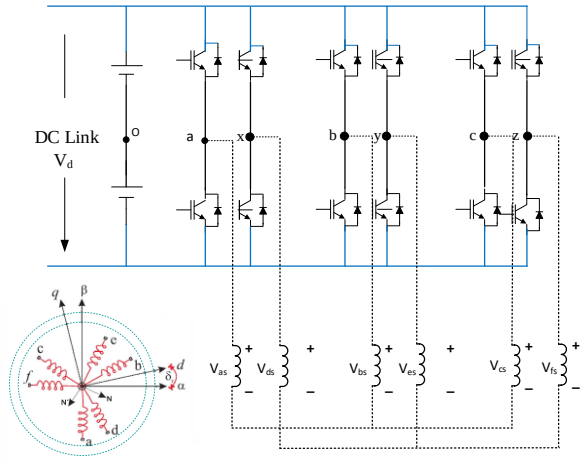

Figure. 1 A general scheme of an SPIM drive

equal to zero. The electromechanical energy conversion only takes place in the DQ subsystem:

$$\begin{bmatrix} V_{sD} \\ V_{sQ} \\ 0 \\ 0 \end{bmatrix} = \begin{bmatrix} R_s + PL_s & 0 & PL_m & 0 \\ 0 & R_s + PL_s & 0 & PL_m \\ PL_m & \omega_r L_m & R_r + PL_r & \omega_r L_r \\ -\omega_r L_m & PL_m & -\omega_r L_m & R_r + PL_r \end{bmatrix} \begin{bmatrix} I_{s\alpha} \\ I_{s\beta} \\ I_{r\alpha} \\ I_{r\beta} \end{bmatrix} \quad (3)$$

where, ω_r is the mechanical angular speed of the rotor, R_s, R_r, L_s, L_r, L_m: stator, rotor resistances and stator, rotor and mutual inductance, respectively.

As these equations implies, the electromechanical conversion, only takes place in the *DQ* subspace and the other subspaces just produce losses. Therefore, the control is based on determining the applied voltage in the *DQ* reference frame. With this transformation, the SPIM control technique is similar to the classical three phase IM FOC. The control for the motor in the stationary reference frame is difficult, even for a three phase IM, so the transformation of SPIM model in a dq rotating reference frame to obtain currents with dc components [1] của 1 is necessary, a transformation matrix must be used to represent the stationary reference fame (D - Q) in the dynamic reference (d - q). This matrix is given:

$$T_{dq} = \begin{bmatrix} \cos(\delta_r) & -\sin(\delta_r) \\ \sin(\delta_r) & \cos(\delta_r) \end{bmatrix} \quad (4)$$

where δr is the rotor angular position referred to the stator as shown in Fig. 1.

The field oriented control (FOC) is the most used strategy in the industrial field. Its objective is to improve the static and dynamic behavior of asynchronous machine unlike the scalar control. It allows decoupling the electromagnetic quantities in order to make the control similar to DC machine, the flux will be controlled by the direct component of the stator current (isd) and the torque by the quadratic component (isq). In this case we obtain:

$$\psi_{rq} = 0; \quad \psi_{rd} = \psi_{rd}$$

Using Eqs. (1) and (4), the new model motor dynamics is described by the following space vector differential equations:

$$\begin{cases} \dfrac{d\omega_r}{dt} = \dfrac{3}{2} P \dfrac{\delta\sigma L_s}{J} (\psi_{rd} i_{sq}) - \dfrac{T_L}{J} - B\omega_r \\ \dfrac{d\psi_{rd}}{dt} = \dfrac{L_m}{\tau_r} i_{sd} - \dfrac{1}{\tau_r} \psi_{rd} \\ L_s \dfrac{di_{sd}}{dt} = -a i_{sd} + L_s \omega_s i_{sq} + b R_r \psi_{rd} + c u_{sd} \\ L_s \dfrac{di_{sq}}{dt} = -a i_{sq} + L_s \omega_s i_{sd} + b_r \omega_r \psi_{rd} + c u_{sq} \end{cases} \quad (5)$$

where, the subscript d and q are the values of the motor parameters in the dq coordinate system, ω_e is synchronous speed, ω_s is slip speed, $\omega_s=\omega_e-\omega_r$, TL is the load torque of the motor, B is the coefficient of friction of the rotor of the motor, J is the moment of inertia of the motor, P is the number of poles, σ is leakage factor:

$$\sigma = 1 - \frac{L_m^2}{L_s L_r}; \; a = \frac{L_m^2 R_r + L_r^2 R_s}{\sigma L_r^2}; c = \frac{1}{\sigma}; b = \frac{L_m^2 R_r}{\sigma L_r^2}$$

3. NN_SM_SC_MRAS speed observer

3.1 NNSM_SC_ MRAS speed observer

In this scheme, the measured stator current components are also used as the reference model of the MRAS observer to avoid the use of a pure integrator and reduce influence of motor parameter variation as in [25-26]. The adaptive model is a two-layer linear NN to estimate the stator current has been trained online by means of a least-squares (**LS**) algorithm. This adaptive model is described by the combined voltage- and current models in the stator reference frame (6)

$$\begin{aligned} T_n \frac{d\hat{i}_{sD}}{dt} &= \frac{1}{x_s \sigma} \left[u_{rD} - r_s i_{sD} \frac{x_m}{x_r} \left(r_r \frac{x_m}{x_r} i_{sD} - \frac{r_r}{x_r} \Psi_{rD} - \omega \Psi_r \right) \right] \\ T_n \frac{d\hat{i}_{sQ}}{dt} &= \frac{1}{x_s \sigma} u_{rQ} - r_s i_{sQ} - \frac{x_m}{x_r} \left(r_r \frac{x_m}{x_r} i_{sQ} - \frac{r_r}{x_r} \Psi_{rQ} + \omega \Psi_{rD} \right) \end{aligned} \quad (6)$$

where, x_s, x_r, x_m: respectively stator, rotor reactances and magnetizing, $T_n=1/2\pi f_{sn}$, f_{sn}: nominal frequency. Eq. (6), Then they been divided by Tn, be re written in the following as:

$$\dot{X} = AX + Bu \tag{7}$$

where: x, u represent the status vectors and input vector, respectively:

$X = \begin{bmatrix} i_{sD} & i_{sQ} \end{bmatrix}^T$; $u = \begin{bmatrix} V_{sD} & V_{sQ} & \hat{\Psi}_{rD} & \hat{\Psi}_{rQ} \end{bmatrix}^T$

$\dot{X} = \begin{bmatrix} \frac{di_{sD}}{dt} & \frac{di_{sQ}}{dt} \end{bmatrix}^T$ [A] and [B] matrices are defined:

$$A = \begin{bmatrix} -\left(1+\frac{x_m^2}{x_r^2}\right)\frac{r_S}{x_S\sigma} & 0 \\ 0 & -\left(1+\frac{x_m^2}{x_r^2}\right)\frac{r_S}{x_S\sigma} \end{bmatrix}; B = \begin{bmatrix} \frac{1}{x_S\sigma} & 0 & \frac{1}{x_S\sigma}\frac{r_r x_m}{x_r^2} & \frac{1}{X_S\sigma}\frac{x_m\omega_r}{X_r} \\ 0 & \frac{1}{x_S\sigma} & \frac{1}{x_S\sigma}\frac{x_m\omega_r}{x_r} & \frac{1}{x_S\sigma}\frac{r_r x_m}{x_r^2} \end{bmatrix}$$

Its corresponding discrete model is, therefore, given by:

$$\hat{X}(k) = e^{[A]T_s} X(k-1) + \left(e^{AT_s} - 1\right) A^{-1} B_u (k-1) \tag{8}$$

where, $e^{\mathbf{A}\,\mathbf{T_s}}$: is generally computed by truncating its power series ex pansion, i.e.,

$$e^{AT_S} = I + \frac{AT_S}{1!} + \frac{A^2T_S}{2!} + \cdots + \frac{A^nT_S}{n!} \tag{9}$$

If n=1, the simple forward Euler method is obtained, which gives the following finite difference Eq. [15-17]

$$\begin{aligned} \hat{i}_{sD}(k) &= w_1\hat{i}_{sD}(k-1) + w_2V_{sD}(k-1) + w_3\hat{\psi}_{rD}(k-1) + w_4\hat{\psi}_{rQ}(k-1) \\ \hat{i}_{sQ}(k) &= w_1\hat{i}_{sQ}(k-1) + w_2V_{sQ}(k-1) + w_3\hat{\psi}_{rQ}(k-1) - w_4\hat{\psi}_{rD}(k-1) \end{aligned} \tag{10}$$

where marks the variables estimated with the adaptive model and is the current time sample. A neural network can reproduce these equations, where are the weights of the neural networks defined as:

$$w_1 = 1 - \frac{T_s r_s}{\sigma L_s} - \frac{T_s L_m^2}{\sigma L_s L_r T_r}; w_2 = \frac{T_s}{\sigma L_s}; w_3 = \frac{T_s L_m}{\sigma L_s T_r}; w_4 = \frac{T_s L_m \hat{\omega}_r}{\sigma L_s L_r} \tag{11}$$

where: $\hat{i}_s(k)$the current variables estimated with the adaptive model and k is the current time sample. An artificial neural network (ANN) can reproduce these equations, where w1, w2, w3, w4 are the weights of the neural networks defined as Eq. (11); Ts is the sampling time for the stator current observer. The ANN has, thus, four inputs and two outputs [25, 26]. In the ANN, the weights w1, w2 and w3 are kept constant to their values computed offline while only w4 is adopted online. These equations are the same as those obtained in [26]. In the scheme is presented in [26], the adaptive model is characterized by the feedback of delayed estimated stator current components to the input of the neural network, which means that the adaptive model employed is in simulation mode. Moreover, the adaptive model is tuned online (training) by means of a BPN algorithm, however, nonlinear in its nature with the consequent drawbacks (local minima, heuristics in the choice of the network parameters, paralysis, convergence problems).

In this LS_SC_MRAS observer proposed, the adaptive model based on the ADALINE has been improved. A linear LS algorithm, which is more suitable than a nonlinear one, like the BPN, is used to reduce the computation effort and overcome some drawbacks, which cause by its inherent nonlinearity. Furthermore, the employment of the adaptive model in prediction mode leads to a quicker convergence of the algorithm, a higher bandwidth of the speed control loop, a better behavior at zero-speed, lower speed estimation errors both in transient and steady-state conditions.

An integration method more efficient than that used in Eq. (12) is the so-called modified Euler integration, which also takes into consideration the values of the variables in two previous time steps [32]. From Eq. (6), the following discrete time equations can be obtained, as shown in Eq. (12). Also, in this case, a neural network can reproduce these equations, where and are the weights of the neural networks defined as Eq. (13). Rearranging Eq. (12), the matrix equation is obtained in prediction mode; see Eq. (14). This matrix equation can be solved by any least-square technique. Eq. (14) Matrix equation (14) can be written: $Ax \approx b$, this is a classical matrix equation of the type, where A is

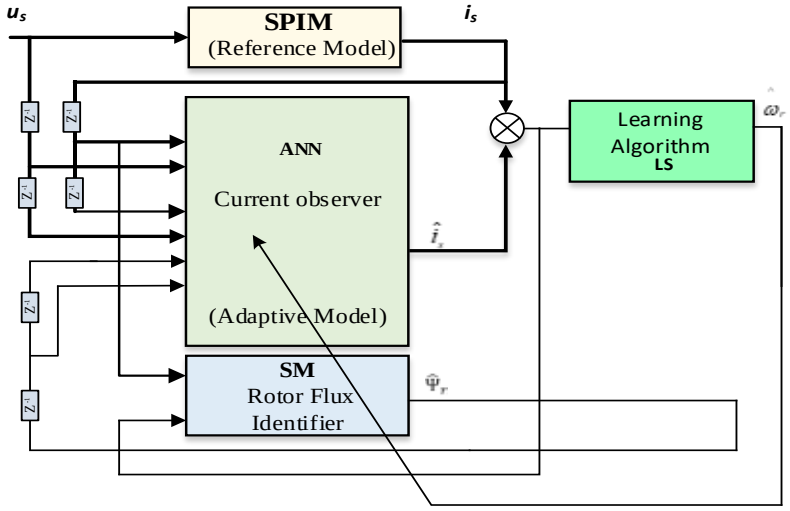

Figure. 2 LS_SC MRAS speed observer

$$\hat{i}_{sD}(k) = w_1 i_{sD}(k-1) + w_2 u_{sD}(k-1) + w_3 \hat{\psi}_{rD}(k-1) + w_4 \hat{\psi}_{rQ}(k-1) + w_5 i_{sD}(k-2) - w_6 u_{sD}(k-2) - w_7 \hat{\psi}_{rD}(k-2) - w_8 \hat{\psi}_{rQ}(k-2)$$

$$\hat{i}_{sQ}(k) = w_1 i_{sQ}(k-1) + w_2 u_{sQ}(k-1) + w_3 \hat{\psi}_{rQ}(k-1) - w_4 \hat{\psi}_{rD}(k-1) + w_5 i_{sQ}(k-2) - w_6 u_{sQ}(k-2) - w_7 \hat{\psi}_{rQ}(k-2) + w_8 \hat{\psi}_{rD}(k-2) \quad (12)$$

where

$$w_1 = 1 - \frac{3TR_s}{2\sigma L_s} - \frac{3TL_m^2}{2\sigma L_r L_s T_r};\ w_2 = \frac{3T}{2\sigma L_s};\ w_3 = \frac{3TL_m}{2\sigma L_r L_s T_r};\ w_4 = \frac{3TL_m}{2\sigma L_r L_s}\omega_r;$$
$$w_5 = \frac{3TR_s}{2\sigma L_s} + \frac{TL_m^2}{2\sigma L_r L_s T_r};\ w_6 = \frac{T}{2\sigma L_s};\ w_7 = \frac{TL_m}{2\sigma L_r L_s T_r};\ w_8 = \frac{TL_m}{2\sigma L_r L_s}\omega_r \quad (13)$$

$$\begin{bmatrix} \frac{3TL_m}{2\sigma L_r L_s}\hat{\psi}_{rQ(k-1)} - \frac{TL_m}{2\sigma L_r L_s}\hat{\psi}_{rQ(k-2)} \\ -\frac{3TL_m}{2\sigma L_r L_s}\hat{\psi}_{rD(k-1)} + \frac{TL_m}{2\sigma L_r L_s}\hat{\psi}_{rD(k-2)} \end{bmatrix} \omega_{r(k-1)} = \begin{bmatrix} \hat{i}_{sD(k)} - w_1 i_{sD(k-1)} - w_2 u_{sD(k-1)} - w_3 \hat{\psi}_{rD(k-1)} - w_5 i_{sD(k-2)} + w_6 u_{sD(k-2)} + w_7 \hat{\psi}_{rD(k-2)} \\ \hat{i}_{sQ(k)} - w_1 i_{sQ(k-1)} - w_2 u_{sQ(k-1)} - w_3 \hat{\psi}_{rQ(k-1)} - w_5 i_{sQ(k-2)} + w_6 u_{sQ(k-2)} + w_7 \hat{\psi}_{rQ(k-2)} \end{bmatrix} \quad (14)$$

called a "data matrix", b is called an "observation vector," and A is the scalar unknown. In this application a classical LS algorithm in a recursive form has been employed; This algorithm is described in detail in [33]. Fig. 2 shows the block diagram of the LS_SC_ MRAS speed observer.

3.2 Rotor speed estimation algorithm

Formula (14), which is a classical matrix equation of the type Ax≈b, where A is called "data matrix", b is called "observation vector," and x is the vector consisting only of the unknown scalar ωr.

Ax≈b is the linear regression problem under hand. All LS problems have been generalized by using a parameterized formulation (generalized LS) of an error function whose minimization yields the corresponding solution. This error is given by:

$$E_{(X)} = \frac{(Ax-b)^T (Ax-b)}{1-\xi+\xi x^T x} \quad (15)$$

where T represents the transpose and ξ is equal to 0.5 for TLS, 1 for DLS and 0 for OLS. Remark that (Ax-b) is the dq axis vector error between the stator current from the reference model (SPIM) and the estimated current by the neural network, i.e,

$$\varepsilon = \begin{bmatrix} \varepsilon_{isD} \\ \varepsilon_{isQ} \end{bmatrix} = \begin{bmatrix} i_{sD} - \hat{i}_{sD} \\ i_{sQ} - \hat{i}_{sQ} \end{bmatrix} \quad (16)$$

This error can be minimized with a gradient descent method. This gives rise to the following speed adaptation law:

The corresponding steepest descent discrete time formula is given by:

$$\hat{\omega}(k+1) = \hat{\omega}(k) - \Delta\omega_r(k) \tag{17}$$

where:

$$\Delta\omega_r = -\eta \frac{dE}{d\omega_r} = \eta\left\{\left(\frac{\left(a(\mathrm{k})^T\omega(\mathrm{k}) - b(\mathrm{k})\right)}{1+\xi+\xi\omega(\mathrm{k})^T\omega(\mathrm{k})}\right)a(\mathrm{k}) + \left(\frac{\left(a(\mathrm{k})^T\omega(\mathrm{k}) - b(\mathrm{k})\right)}{1+\xi+\xi\omega(\mathrm{k})^T\omega(\mathrm{k})}\right)^2 \xi\,\hat{\omega}_r(k)\right\} \tag{18}$$

we get the following modifed equation:

$$\hat{\omega}_r(k+1) = \hat{\omega}_r(k) - \eta\gamma(k)a(k) + [\xi\eta\gamma^2(k)\hat{\omega}_r(k)] \tag{19}$$

where: $\gamma(k) = \dfrac{a(\mathrm{k})^T\omega_r(\mathrm{k}) - b(\mathrm{k})}{1+\xi+\xi\omega_r(\mathrm{k})^T\omega_r(\mathrm{k})}$

η is the learning rate, ai(k) is the row of A fed at instant k, ξ is equal 0 for OLS.

3.3 Rotor flux estimation and stability analysis of observer

Consider a non-linear system described by:

$$\begin{cases} \dot{Z} = F(\omega_r)Z + G(u, \omega_r, Z) \\ y = CZ \end{cases} \tag{20}$$

where:

$$y = z_1 = \begin{bmatrix} i_{sD} \\ i_{sQ} \end{bmatrix}; z_2 = \begin{bmatrix} \varphi_{rD} \\ \varphi_{rQ} \end{bmatrix}; u = \begin{bmatrix} u_{sD} \\ u_{sQ} \end{bmatrix};$$

$$F_1(\omega_r) = \begin{bmatrix} \dfrac{K}{T_r} & K\omega_r \\ -K\omega_r & \dfrac{K}{T_r} \end{bmatrix}; K = \frac{L_m}{\sigma L_r L_s}; \sigma = 1 - \left(\frac{L_m^2}{\sigma L_r L_s}\right)$$

$$g_1(u, \omega_r, z_1) = \begin{bmatrix} -\gamma i_{sD} + \left(\dfrac{1}{\sigma L_s}\right)u_{sD} \\ -\gamma i_{sQ} + \left(\dfrac{1}{\sigma L_s}\right)u_{sQ} \end{bmatrix}; \gamma = \left(\frac{R_s}{\sigma L_s}\right) + \left(R_r\frac{L_m^2}{\sigma L_r L_s}\right)$$

$$g_2(u, \omega_r, z_2) = \begin{bmatrix} \left(\dfrac{L_m}{T_r}\right)i_{sD} - \left(\dfrac{1}{T_r}\right)\varphi_{rD} - \omega_r\varphi_{rQ} \\ \left(\dfrac{L_m}{T_r}\right)i_{sQ} - \left(\dfrac{1}{T_r}\right)\varphi_{rQ} + \omega_r\varphi_{rD} \end{bmatrix};$$

If the system is observable, the objective of the observer is to give the best state variables. From the measurement of output y and input u, the observer is defined by the follow structure:

$$\dot{\hat{z}} = F(\omega_r)\hat{z} + G(u, \omega_r, \hat{z}) + \Lambda I_s \tag{21}$$

where Λ is the gain matrix and *Is* is a vector defined by:

$$I_s = \begin{bmatrix} sat(s_1) & sat(s_2) \end{bmatrix}^T \tag{22}$$

with S is the slide surface of the observer is defined as following:

$$S = \begin{bmatrix} s_1 & s_2 \end{bmatrix}^T = \begin{bmatrix} i_{sD} - \hat{i}_{sD} & i_{sQ} - \hat{i}_{sQ} \end{bmatrix}^T \tag{23}$$

Subtracting Eq. (20) and (21) gives:

$$\dot{\varepsilon} = \left[F(\omega_r)z - F(\omega_r)\hat{z} + G(u, \omega_r, z) - G(u, \omega_r, \hat{z})\right] - \Lambda I_s \tag{24}$$

With ε is the error vector defined by:

$$\varepsilon = \begin{bmatrix} \varepsilon_1 & \varepsilon_2 & \varepsilon_3 & \varepsilon_4 \end{bmatrix}^T = \begin{bmatrix} i_{sD} - \hat{i}_{sD} & i_{sQ} - \hat{i}_{sQ} & \varphi_{rD} - \hat{\varphi}_{rD} & \varphi_{rQ} - \hat{\varphi}_{rQ} \end{bmatrix}^T \tag{24}$$

The aim of this section is to estimate the rotor flux components based on the stator currents and voltages that are easily measurable. From Eq. (6), the flux estimation algorithm based on sliding-mode theory is defined:

$$\begin{cases} \dot{\hat{\varphi}}_{rD} = \left(\dfrac{L_m}{T_r}\right)i_{sD} - \left(\dfrac{1}{T_r}\right)\hat{\varphi}_{rD} - \hat{\omega}_r\hat{\varphi}_{rQ} + \Lambda_{\varphi rD}I_s \\ \dot{\hat{\varphi}}_{rQ} = \left(\dfrac{L_m}{T_r}\right)i_{sQ} - \left(\dfrac{1}{T_r}\right)\hat{\varphi}_{rQ} + \hat{\omega}_r\hat{\varphi}_{rD} + \Lambda_{\varphi rQ}I_s \end{cases} \tag{25}$$

From (21), the dynamic of the estimation error is given by:

$$\begin{cases} \dot{\varepsilon}_1 = \left(\dfrac{K}{T_r}\right)\varepsilon_3 + K\omega\varepsilon_4 - \Lambda_i I_s \\ \dot{\varepsilon}_2 = \left(\dfrac{K}{T_r}\right)\varepsilon_4 - K\omega\varepsilon_3 - \Lambda_i I_s \\ \dot{\varepsilon}_3 = \left(-\dfrac{1}{T_r}\right)\varepsilon_3 - \omega\varepsilon_4 - \Lambda_\varphi I_s \\ \dot{\varepsilon}_4 = \left(-\dfrac{1}{T_r}\right)\varepsilon_4 + \omega\varepsilon_3 - \Lambda_\varphi I_s \end{cases} \tag{26}$$

By defining Lyapunov function as:

$$V = \frac{1}{2} S^T S \tag{27}$$

Whose time derivative is,

$$\frac{dV}{dt} = S^T \frac{dS}{dt} = \begin{bmatrix} \varepsilon_1 & \varepsilon_2 \end{bmatrix} \begin{bmatrix} \left(\frac{K}{T_r}\right)\varepsilon_3 + K\omega\varepsilon_4 - \Lambda_i I_s \\ \left(\frac{K}{T_r}\right)\varepsilon_4 - K\omega\varepsilon_3 - \Lambda_i I_s \end{bmatrix} \tag{28}$$

when the currents trajectory reaches the sliding surface $\varepsilon_1=\varepsilon_2=0$, the observer error dynamics given by (22) behaves, in the sliding-mode as a reduced order system governed only by the roto flux error, because $\varepsilon_{is} = \dot{\varepsilon}_{is} = 0$

In order to demonstrate the stability of the previous system, the following Lyapunov function candidate is proposed:

$$V = \frac{1}{2}\begin{bmatrix} \varepsilon_3 & \varepsilon_4 \end{bmatrix}\begin{bmatrix} \varepsilon_3 & \varepsilon_4 \end{bmatrix}^T \tag{29}$$

The time derivative of the Lyapunov function candidate is:

$$\frac{dV}{dt} = \begin{bmatrix} \varepsilon_3 & \varepsilon_4 \end{bmatrix} \begin{bmatrix} \left(-\frac{1}{T_r}\right)\varepsilon_3 - \omega\varepsilon_4 - \Lambda_\varphi I_s \\ \left(-\frac{1}{T_r}\right)\varepsilon_4 + \omega\varepsilon_3 - \Lambda_\varphi I_s \end{bmatrix} \tag{30}$$

When sliding takes place:

$$\Lambda_\varphi = \begin{bmatrix} \Lambda_{\varphi rd} & 0 \\ 0 & \Lambda_{\varphi rq} \end{bmatrix} = -\Lambda_v \begin{bmatrix} \frac{1}{T_r} & \omega \\ -\omega & \frac{1}{T_r} \end{bmatrix} \begin{bmatrix} \varepsilon_3 \\ \varepsilon_4 \end{bmatrix} = -\Lambda_v \Gamma \begin{bmatrix} \varepsilon_3 \\ \varepsilon_4 \end{bmatrix} \tag{31}$$

Choose $\Lambda = \Delta\Gamma^{-1}$ where $\Delta = \begin{bmatrix} \delta_1 & -\omega_r \\ \omega_r & \delta_2 \end{bmatrix}$ and δ_1, δ_2 are positive design constants.

Note that $\det(\Gamma(\omega_r)) \neq 0$ for all $\omega_{r\ and}$ so the inverse always exists. From Eq. (31), when sliding takes place, substituting from Eq. (26) yields:

$$\begin{bmatrix} \dot{\varepsilon}_3 \\ \dot{\varepsilon}_4 \end{bmatrix} = \left\{ \begin{bmatrix} -\frac{1}{T_r} & -\omega \\ \omega & -\frac{1}{T_r} \end{bmatrix} - \Delta\Gamma^{-1}\Gamma \right\} \begin{bmatrix} \varepsilon_3 \\ \varepsilon_4 \end{bmatrix} = \begin{bmatrix} \left(-\frac{1}{T_r}\right) - \delta_1 & 0 \\ 0 & \left(-\frac{1}{T_r}\right) - \delta_2 \end{bmatrix} \begin{bmatrix} \varepsilon_3 \\ \varepsilon_4 \end{bmatrix} \tag{32}$$

This is, the flux observer error converges to zero with exponential rate of convergence.

4. Simulink and Discussion

In order to verify and evaluate the performance of the SC_MRAS observer using NN and SM a sensorless vector control of SPIM drive system, as shown in Fig. 6 has been simulated at different speed ranges through Matlab simulation software, specially surveyed at low speed range. Tests in this section are conducted based on recommended benchmark tests [23-24], [29-31]. SPIM parameters: 1HP, 220V, 50 Hz, 4 pole, 1450 rpm. Rs = 10.1Ω, Rr = 9.8546Ω, Ls = 0.833457 H, Lr = 0.830811 H, m = 0.783106H, Ji = 0.0088 kg.m2. The simulation results show the performance of the proposed estimator in different conditions: during speed reversal, low speed operation, ramp response, effect of parameter variation and during the regenerating mode operation.

4.1 Dynamic performance

In this first part, the dynamic performance of the drive and observer have been verified by the tests are conducted based on recommended Benchmark tests in [23, 27]. Test 1 presents rapid transitions and operating areas at large and zero speeds, Test 2 consists of low and very low speed operation and reversal. In Test 1, the reference speed is imposed from zero increased to 125 rad/s and constant up to 4s. Then, it is reduced to zero. Between 2,5 s and 4,8 s, a quasi-symmetric velocity profile is imposed in the opposite rotational direction, defining a second area of critical operating at -125 rad/s between 5s and 6s and constant up to 10s. Then, the motor speed is again reduced to zero. Rated load is applied at 2s and rejected at 4s, at 7s and rejected at 9s, respectively with –rated load is applied. The application and removal of a torque load at the moments will also assess the impact of this type of disturbance at the high speed operations. The results in Fig.4 show the speed responses, the speed estimation error, the stator current and torque during test 1. From these simulation results show that although surveyed with larger speed range compare to in [27] (Fig. 2 (a)), the estimation performance of NNSM_SC_MRAS observer is very good at high,

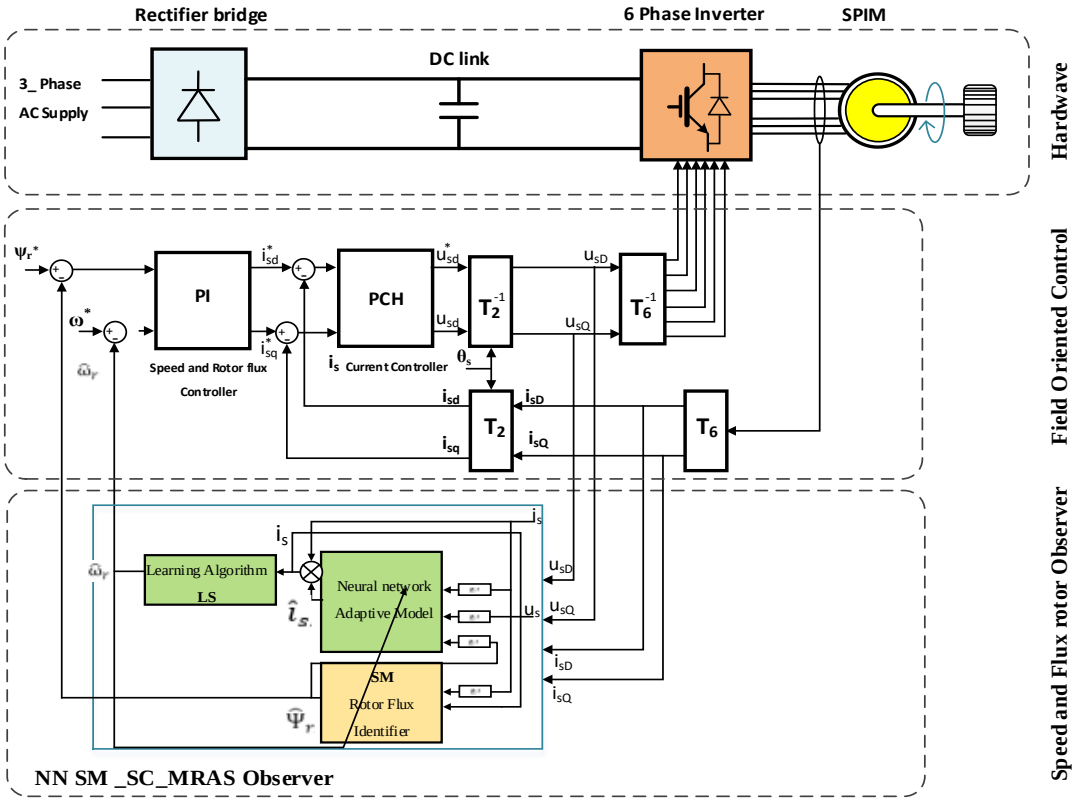

Figure. 3 Sensorless vector control of SPIM drive using LS_SC_MRAS observer

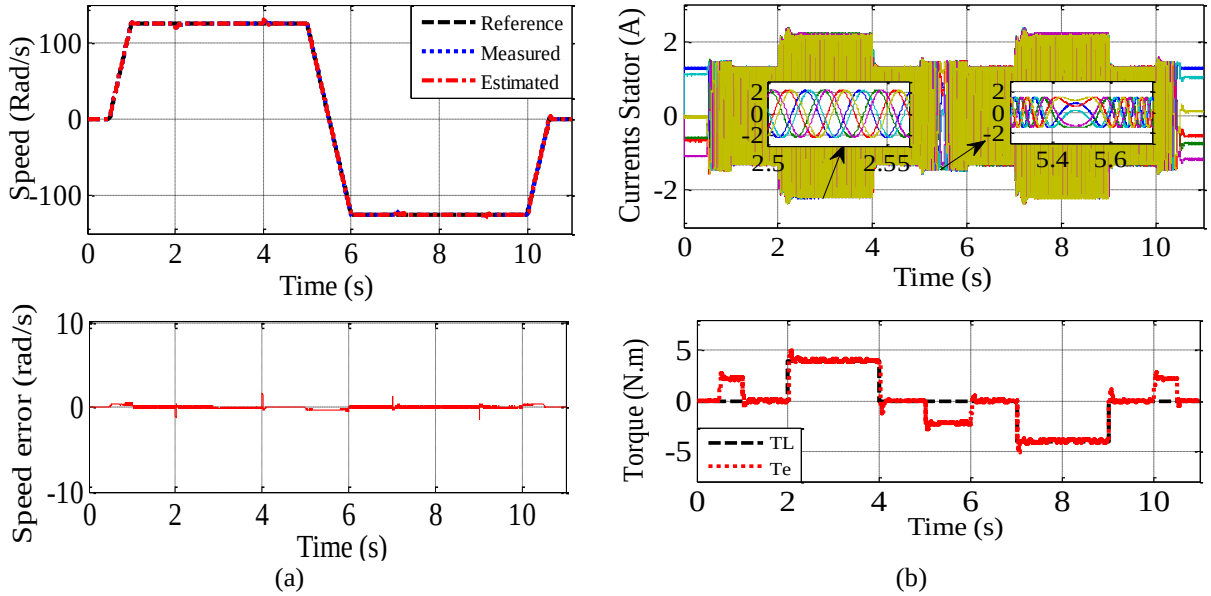

Figure. 4 The performance of NNSM_ SC_MRAS obsever during high speed reversal: (a) speed responses and error, respectively and (b) Stator current phase A and torque response

low and zero speed and reversal. The speed estimation error is the estimated speed perfectly follows the rotor speed with good behavior in terms of tracking and disturbance rejection. The proposed schemes in [23, 27]; and NNSM_SC_MRAS scheme, the speed reversal is accomplished in less than 1s and that the torque response is instantaneous. The speed error is maximum at zero crossing and during the speed transient and it is about as much as 0.105 rad/s in NNSM_SC_MRAS observer, 0.5 rad/s in the proposed observer [23] (Figs. 4, 5, 6). Furthermore, a speed reversal from 5 rad/s to -5 rad/s and 8 rad/s, at 25%load has been performed for testing the dynamic performances of the drive using NNSM-SC_MRAS at low speed. Fig. 5 shows the speed and torque response of NNSM_SC_MRAS drive is very quick and that after few oscillations it converges to the reference value.

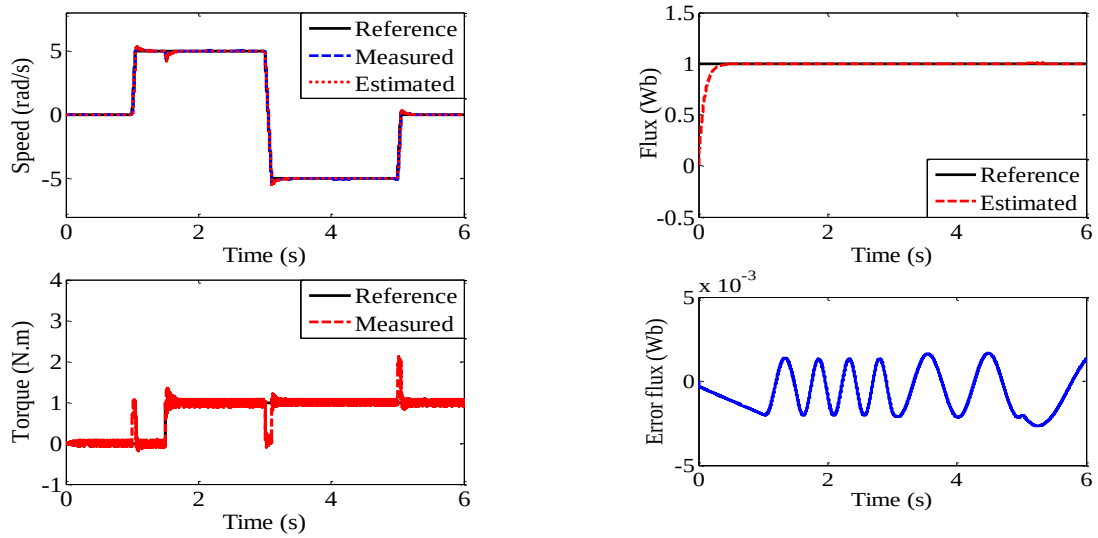

(a) (b)

Figure. 5 The performance of NNSM_ SC_MRAS obsever during low speed reveral: (a) speed responses and (b) rotor flux responses and error, respectively, torque responses

We observe very small oscillations during transients and very low orientation errors in the two critical areas of the proposed observer. The application 25% load at 1.75 s and keep constant in the whole time of the remaining survey will also assess the impact of this type of regenerating mode operation. Using SM to identify rotor flux will avoid the instability in the regenerating mode, the survey time from 3s to 6s, demonstrates this.

From two above tests, the speed estimation performance of the proposed observer, which are surveyed in the case of very high dynamics in Fig. 4 and Fig. 5 are very well, the maximum overshoot and the speed estimation error obtained with the NNSM_SC_ MRAS observer are lower than the corresponding one with the observer [23, 27] and [20]. The torque response obtained with this proposed observer is very smooth, while the corresponding one obtained with the proposed observer in [20] is much affected by ripple ([20], Fig. 3 (b), and 4 (b)), [27] the performance of the observer in case of low speed reversal is not surveyed]. The performance of the proposed scheme is very stable and very good in wide speed range.

4.2 The performance of proposed observer in very low speed ranges

In this test, the performance of the speed estimation has been verified in the very low and zero speed ranges based on proposed benchmark tests [24]. The drive has been given a speed reference step from 15 rad/s to zero then increase to 15 rad/s, 3 rad/s steps, 25% load applied at 2.5s and rejected at 15s. Fig 6 a,b show the speed responses of proposed SC_MRAS at no load and 25% load, respectively. The simulink results show that no instability phenomena occur at low and zero speed range, the speed estimated error is not significantly. In contrast, with a proposed observer in [24] (Figs. 7 and 8) shows instability phenomena, the estimated error increase at low and zero speed range. Another survey also is carried out to justify the effectiveness of the proposed method in the low speed region by providing the sets of ramp speed reference operation from 0 to ±15 rad/s working with rated load, this test is conducted based on recommended benchmark tests [29]. In any case, better results in the estimation accuracy at low speeds are to be expected with both NNSM_SC_ MRAS and MRAS observers in [29]. The simulink results in Fig. 7 and in [29] (Fig. 4) show the performances of both the estimators for triangular speed command in both the forward and reverse motoring modes at rated load torque are very well. However, the zoom of speed figure shows the speed deviation of NNSM_SC_MRAS estimator is less than the proposed MRAS estimator in [29]. For the MRAS observer, which is proposed in [29], the speed error the error between estimated, measured speed and reference higher, the convergence time of the estimated and measured speed to reference speed value are longer (Fig 4b) than NNSM_SC_MRAS obeserver. Using SM to estimate the rotor flux gives stability in the speed reveral, is not disturbed.

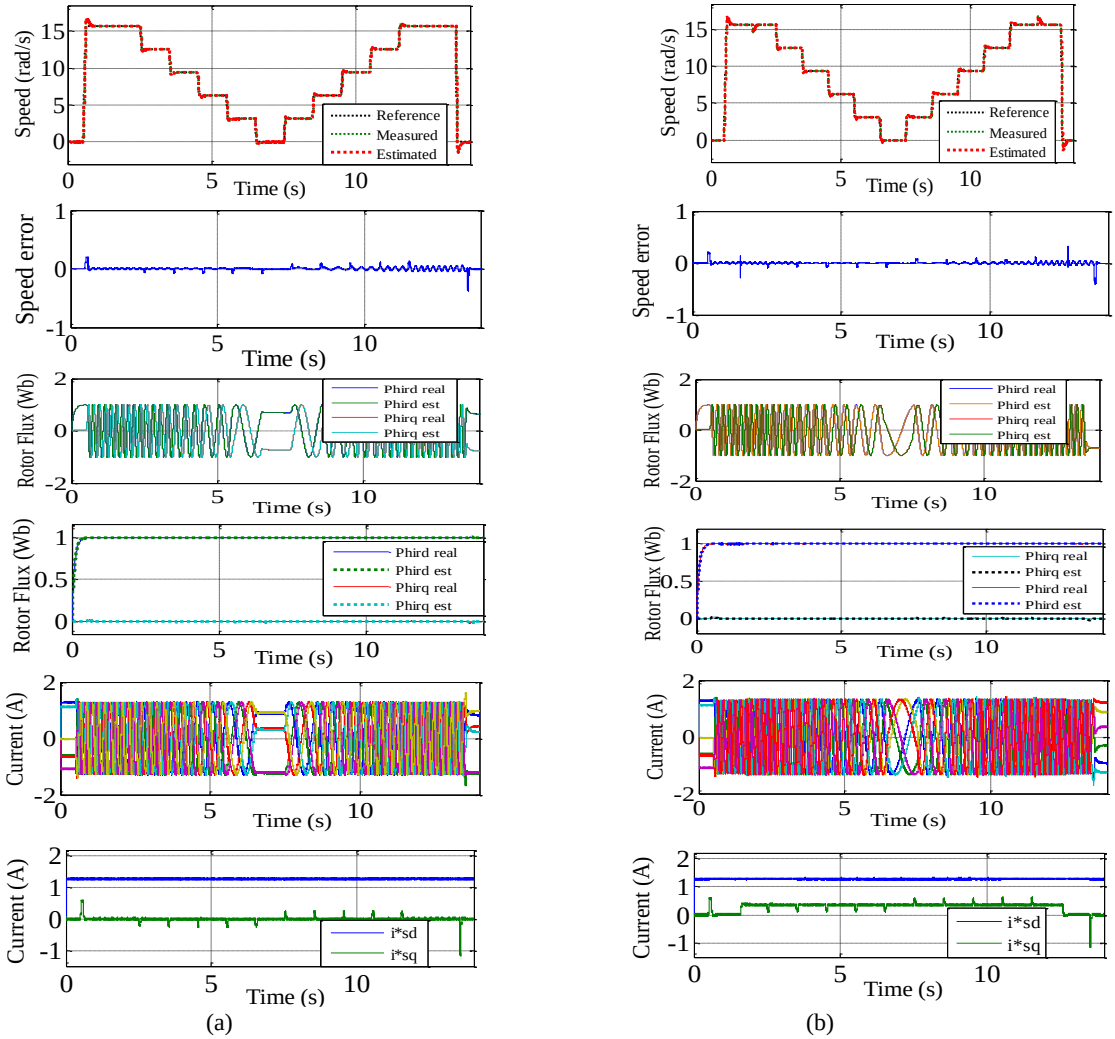

Figure. 6 The speed of the SPIM in very low operation speed region using: (a) no load and (b) 25% load

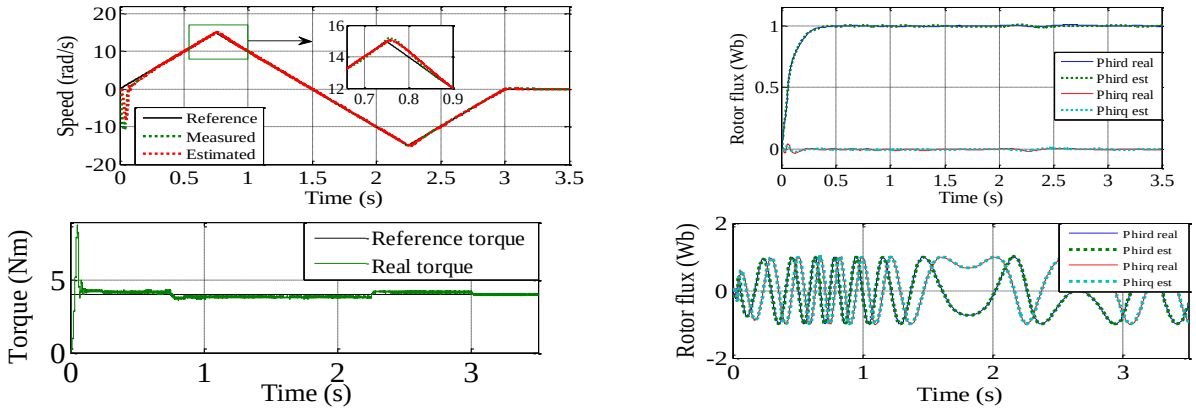

Figure. 7 The speed of the SPIM in very low speed ramp response

4.3 Dynamic performance

The purpose of this test is to verify the speed estimation performance of the proposed MRAS observers for motor parameter variation. The drive and observer have been verified based on recommended benchmark tests in [23] but extending survey additionally case the resistance values increase 50%. Fig. 8 shows the performance of the observer when Rs variations. Rs is increased 30% and 50%, load is applied at 2s. The reference speed is increased from zero to 20 rad/s, then is reduced to 12 rad/s to 7 rad/s to zero. The stable operation and

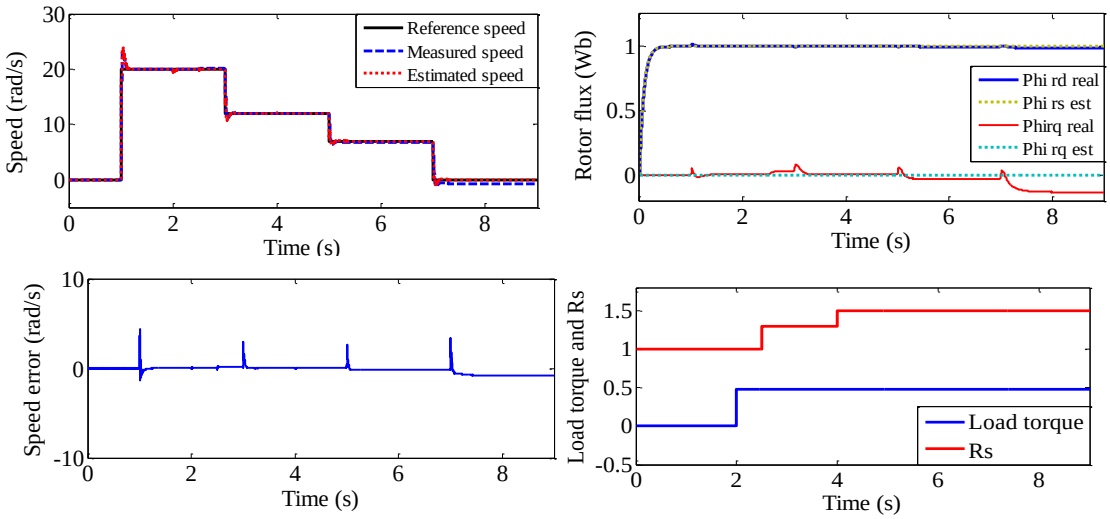

Figure 8. The performance of the NNSM_SC_ MRAS observer when Rr variations: (a) estimated speed, (b) speed error, (c) estimated rotor flux, and (d) load torque

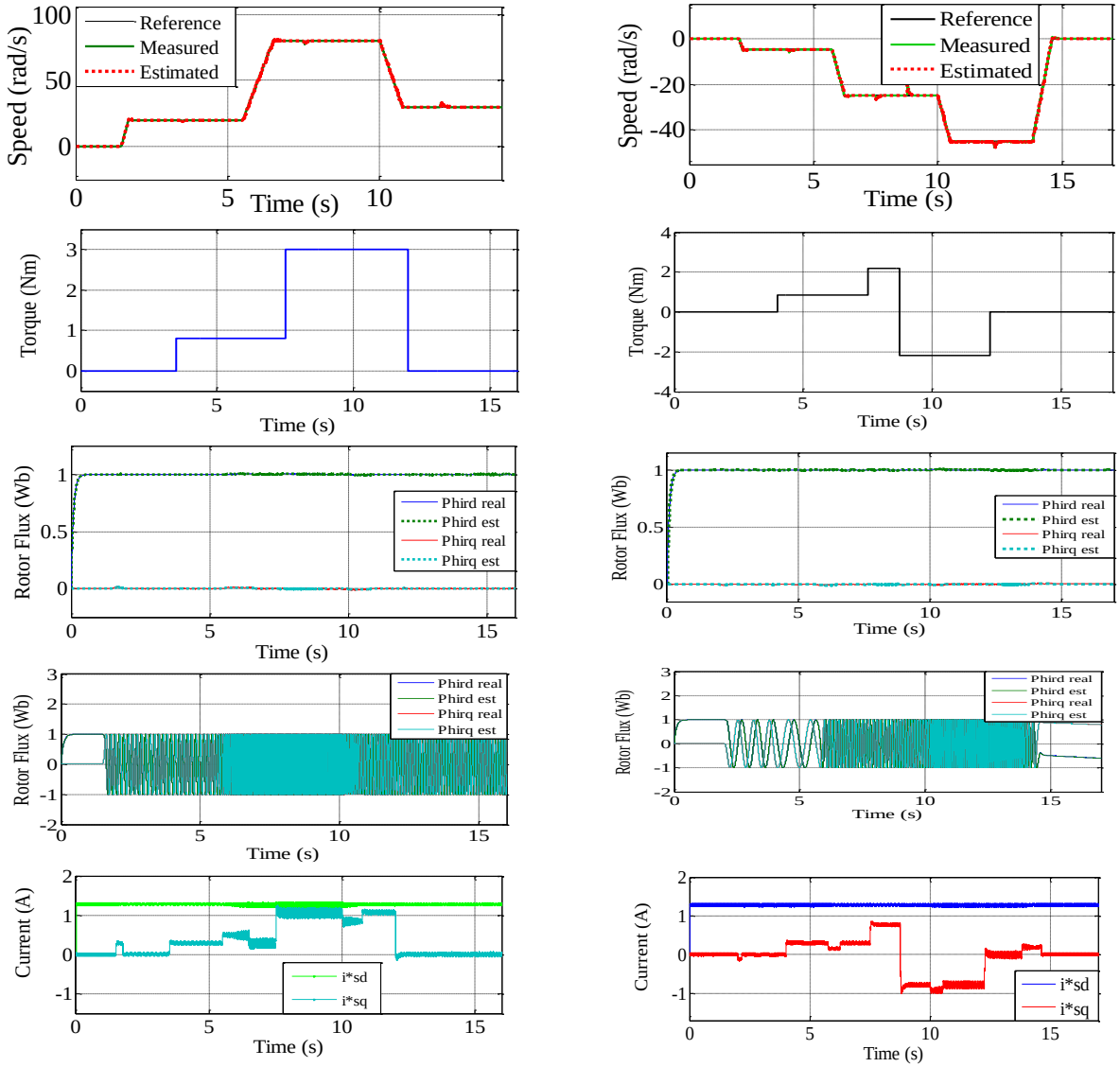

Figure. 9 Load perturbations and the regenerating mode operation test: (a) simulated responses to variation in speed and load demands for motoring operation and (b) simulated responses to variation in negative speed and load demands for both motoring and regenerative operation

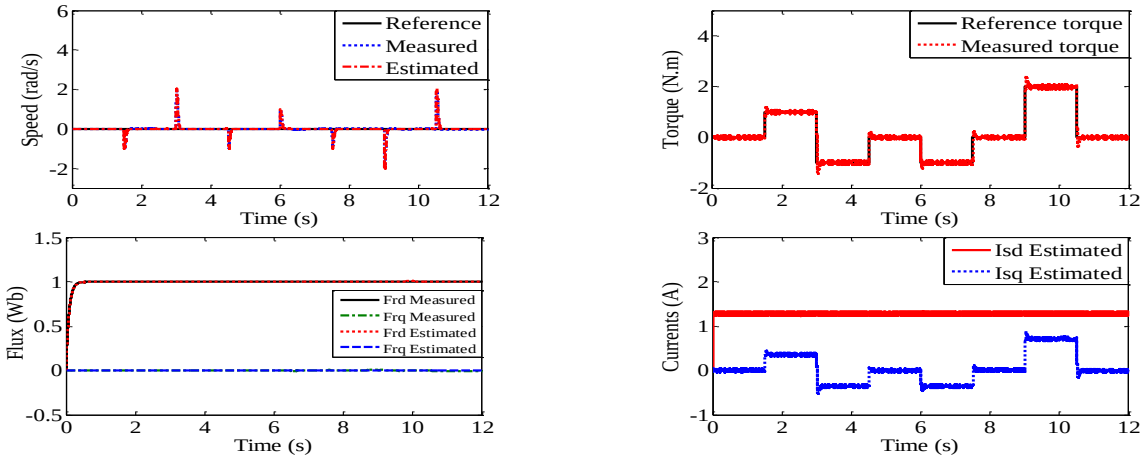

Figure. 10 Load perturbations test at zero speed, load torque various

oscillating speed performance of the NNSM_ SC_MRAS observer (Fig. 8) and proposed observer in [23] (Fig.10) obtained are very well with Rs increases 30%. For the proposed SC_MRAS, when increasing Rs up to 50%, its performance is still well, the speed and rotor flux estimation error only increase when observer working at zero speed region. (the performance of the observer with the Rs variation increased 50% were not shown in [23])

4.4 Load perturbations and the regenerating mode operation

The robustness of the speed estimation of the observer to a sudden torque perturbation has been surveyed in this test. It was carried out to prove the behavior of the proposed scheme when load torque variations. Fig. 9a shows the speed estimation performance of NNSM_SC_MRAS observer and drive system with the rotor speed responses of the proposed MRAS observer to a variation in load torque and rotor speed for the motoring regions of operation to a speed demand of 20 rad/s increase to 80 rad/s, then reducing to 30 rad/s, 25% load applied at 3.5s, increasing to 75% load at 7.5s, and reducing to zero at 12s. Fig. 9b shows the regenerating operation regions, a speed demand of -5 rad/s, 25 rad/s with 25% load and 55% load applied at 4s, 7.5s before a severe load torque reversal from 55% to -55% occurs at 8.75 s. These result shows the proposed improved current MRAS scheme given better the transient and steady state performance than to the TMRAS in [24] (Fig.9; 10). This is due to the stator current based scheme is not directly affected by stator voltage, in contrast, TMRAS scheme in [24] for rotor flux estimation is affected by this voltage hence the proposed scheme has better performance especially at low speed with less steady state error. In Fig 14 from result of the flux and current responses show the proposed schemes capability of handling regenerative operation and large load changes better [24].

The behavior of the proposed scheme with rotor speed was kept by zero during test, the speed estimation performance for load disturbance rejection at +25% load in time 1.5s- 3s; -25% load in time 3s-4.5s; and 6 s-7.5s; 75% load in 9s- 10.5. Fig. 15 show the reference, measured, and estimated speed, these results show that the speed responses of the drive using the proposed NN SC_MRAS observer occurs immediately when the torque steps are given (Fig. 10). The small oscillations occur when 75% load rejected, however, very low estimation errors of the proposed observer, even during the speed transient that caused by the torque step, the estimated speed follows the real speed is very well. Comparing these results with the result in [24] (Fig. 12) is easily seen using SC_MRAS based observer with the improved rotor flux identify using SM given the performance better. in [24] speed and rotor flux estimation error increase high when applying load, on the contrary, the NNSM_SC_MRAS scheme operates very well in whole survey range.

5. Conclusion

This paper has presented NNSM_SCMRAS speed observer for high performance SPIM drives using NN and SM. It led evaluating and improving the MRAS observer shown in [26]. The new SC_MRAS speed observer using the LS algorithm instead BPN algorithm [35] to can both reducing the computation effort and still improving the performance of proposed observer. In addition, the adaptive model based on NN is implement in prediction mode also increase accuracy and stability both in transient and stable state operations.

Especially, in this proposed observer, the rotor flux is identified based on adaptive SM technique. The improvement of Rotor Flux Estimation for SC_MRAS-Based Sensorless SPIM drives help to eliminate the disadvantages in SC_MRAS based observer such as stator resistance sensitivity, and flux open loop integration which may cause dc drift and initial condition problems, therefore, enhancing the rotor flux estimation, speed estimation and control accuracy at very low and zero stator frequency operation help improve the overall observer and drive system performance. The theoretical analysis is validated by simulation tests of the sensorless SPIM drive system under different operating conditions and these simulation results are given to compare the performance of the proposed observer with recent proposed observer [23, 24, 27, 29, 31]. From the analysis and comparison data in section 2 and 3 have proven that the proposed NN_SM_SC_MRAS observer are simpler, require lower computation effort but it' estimated speed is quicker convergence time, better dynamic performances; lower estimation errors both in transient and steady-state operation. The terms of accuracy of the NN_SM_SCMRAS observers is quite high and it is robustness against motor parameter variations, especially at low and zero speed region.

References

[1] E. Levi, "Multiphase electric machines for variable-speed applications", *IEEE Transactions on Industrial Electronics*, Vol.55, No.5, pp.1893 – 1909, 2008.

[2] R. Kianinezhad, B.N. Mobarakeh, L. Baghli, F. Betin, and G.A. Capolino, "Modeling and Control of Six-Phase Symmetrical Induction Machine Under Fault Condition Due to Open Phases", *IEEE Trans. Ind. Elec*, Vol. 55, No.5, pp. 1966-1977, 2008.

[3] H. Kubota, K. Matsuse, T. Nakano, "DSP-based speed adaptive flux observer of induction motor", *IEEE Trans. Ind. Appl*, Vol.29, No. 2, pp. 344-348, 1993.

[4] S. Yin, S. X. Ding, X. C. Xie, and H. Luo, "A Review on Basic Data Driven Approaches for Industrial Process Monitoring", *IEEE Trans. Ind. Electron*, Vol.61, No.11, pp.6418-6428, 2014.

[5] S. Hussain and M.A. Bazaz, "Neural network observer design for sensorless control of induction motor drive", *IFAC-Papers OnLine*, Vol. 49, pp.106-111, 2016.

[6] R.Vieira and C. Gastaldini, "Azzolin R, Gründling. Discrete-time sliding mode speed observer for sensorless control of induction motor drives", *IET Electr. Power Appl*, Vol.6, No. 9, pp. 681- 688, 2012.

[7] S. Jafarzadeh and C. Lascu, "Fadali. State estimation of induction motor drives using the unscented Kalman filter", *IEEE Trans. Ind. Electron*, Vol.59, No.11, pp. 4207- 4216, 2012.

[8] C. Schauder, "Adaptive speed identification for vector control of induction motors without rotational transducers", *IEEE Trans. Ind. Appl*, Vol.59, No.11, pp. 4207- 4216, 2012.

[9] AV. RaviTeja, C. Chakraborty, S. Maiti, and Y. Hori, "A new model reference adaptive controller for four quadrant vector controlled induction motor drives", *IEEE Trans. Ind. Electron*, Vol.59, No.10, pp. 3757-3767, 2012.

[10] S. Maiti, V. Verma, C. Chakraborty, and Y. Hori, "An adaptive speed sensorless induction motor drive with artificial neural network for stability enhancement", *IEEE Trans. Ind. Inf*, Vol. 8, No.4, pp. 757-766, 2012.

[11] Y.B. Zbede, S.M. Gadoue, and D.J. Atkinson, "Model Predictive MRAS Estimator for Sensorless Induction Motor Drives", *IEEE Trans. Ind. Electronics*, Vol. 63, No.6, pp. 3511-3521, 2016.

[12] B. Abdelhak and B. Bachir, "A High Gain Observer Based Sensorless Nonlinear Control of Induction Machine", *International Journal of Power Electronics and Drive System*, Vol.5, No.3, pp. 305-314, 2015.

[13] A. Flah and S. Lassaad, "An adaptive high speed PMSM control for electric vehicle application. Journal of Electrical Engineering," Vol. 12, No. 3, pp. 165-177, 2012.

[14] G. Foo and M.F. Rahman, "Sensorless sliding-mode MTPA control of an IPM synchronous motor drive using a sliding-mode observer and HF signal injection", *IEEE Trans. Ind. Electron*, Vol. 57, No. 4, pp.1270-1278. 2010.

[15] A. Flah, M. Novak, and S. Lassaad, "An Improved Reactive Power MRAS Speed Estimator with Optimization for a Hybrid Electric Vehicles Application", *J. Dyn. Syst. Meas. Control*, Vol.140, No.6, pp. 016 - 061, 2018.

[16] J. Holtz, "Sensorless control of induction motor drives", In: *Proc. of the IEEE*, Vol. 90, No. 8, pp. 1359-1394, 2002.

[17] A. Flah, L. Sbita, and M. B. Hamed, "Online MRAS-PSO PMSM parameters estimation", *International Review on Modelling and Simulations*, Vol. 4, No.3, pp. 980-987, 2011.

[18] J. Holtz and J. Quan, "Drift and parameter compensated flux estimator for persistent zero stator frequency operation of sensorless controlled induction motors", *IEEE Trans. Ind. Appl.*, Vol. 39, No. 4, pp. 1052-1060, 2003.

[19] C.B. Regaya, F. Farhani, A. Zaafouri, and A. Chaari, "A novel adaptive control method for induction motor based on Backstepping approach using dSpace DS 1104 control board", *Mechanical Systems and Signal Processing*, Vol. 100, pp, 466-481, 2018.

[20] M. Horch, A. Boumediene, and L. Baghli, "MRAS-based Sensorless Speed Integral Backstepping Control for Induction Machine, using a Flux Backstepping Observer", *International Journal of Power Electronics and Drive System*, Vol. 8, No. 4, pp.1650-1662, 2017.

[21] M. Jannati, N.R.N. Idris, and M.J.A. Aziz, "Indirect Rotor Field-Oriented Control of Fault-Tolerant Drive System for Three-Phase Induction Motor with Rotor Resistance Estimation Using EKF", *TELKOMNIKA Indonesian Journal of Electrical Engineering*, Vol.12, No. 9, pp. 6633 – 6643, 2014.

[22] M. Jannati, S.H. Asgari, N.R.N Idris, and M.J.A. Aziz, "Speed Sensorless Direct Rotor Field-Oriented Control of Single Phase Induction Motor Using Extended Kalman Filter", *International Journal of Power Electronics and Drive System*, Vol. 4, No. 4, pp. 430-438, 2014.

[23] Benlaloui, D. Drid, L.C. Alaoui, and M. Ouriagli, "Implementation of a New MRAS Speed Sensorless Vector Control of Induction Machine", *IEEE Transactions on Energy Conversion*, Vol. 30, No. 2, pp.588-595, 2015

[24] N. Smith, S.M. Gadoue, and J.W. Finch, "Improved Rotor Flux Estimation at Low Speeds for Torque MRAS-Based Sensorless Induction Motor Drives", *IEEE Transactions on Energy Conversion*, Vol. 31, No. 1, pp. 270-282, 2016.

[25] N.T. Pham, D.P. Nguyen, K.H. Nguyen, and N.V. Nguyen, "An Improved Neural Network SC_MRAS Speed Observer in Sensorless", *WSEAS Transactions on Systems and Control*, Vol.13, Art. #39, pp. 364-374, 2018.

[26] S.M. Gadoue, D. Giaouris, and J.W. Finch, "Stator current model reference adaptive systems speed estimator for regenerating-mode low-speed operation of sensorless induction motor drives", *IET Electr. Power Appl*, Vol. 7, No. 7, pp. 597- 606, 2013.

[27] G. Tarchała and T.O. Kowalska, "Equivalent Signal Based Sliding Mode Speed MRAS-type Estimator for Induction Motor Drive Stable in the Regenerating", *IEEE Trans. Ind. Electron*, Vol. 65, No. 9, pp. 6936- 6947, 2018.

[28] N.T. Pham, D.P. Nguyen, K.H. Nguyen, and N.V. Nguyen, "A Novel Neural Network SC_MRAS Based Observer for High-Performance SPIM Drives", *International Journal of Intelligent Engineering and Systems*, Vol.11, No.6, pp. 95-107, 2018

[29] A. Pal, S. Das, and A.K. Chattopadhyay, "An Improved Rotor Flux Space Vector Based MRAS for Field Oriented Control of Induction Motor Drives", *IEEE Transactions on Power Electronics*, Vol. 33, No. 6, pp. 5131-5141, 2018.

[30] B.G. Tarchała and T.O. Kowalska, "Equivalent Signal Based Sliding Mode Speed MRAS-type Estimator for Induction Motor Drive Stable in the Regenerating", *IEEE Trans. Ind. Electron*, Vol. 65, No. 9, pp. 6936- 6947, 2018.

[31] M. Horch, B. Abdelmadjid, and B. Lotfi, "MRAS-based Sensorless Speed Integral Backstepping Control for Induction Machine, using a Flux Backstepping Observer", *International Journal of Power Electronics and Drive System*, Vol. 8, No. 4, pp.1650-1662, 2017.

[32] J. H. Matheus and K. D. Fink, "Numerical Methods Using Matlab", *4th ed. Upper Saddle River, NJ: Prentice-Hall*, 2004.

[33] G. Cirrincione, M. Cirrincione, J. Hérault, and S.V. Huffel, "The MCA EXIN neuron for the minor component analysis: Fundamentals and comparisons", *IEEE Trans. Neural Netw.*, Vol. 13, Nol. 1, pp. 160-187, 2002.